

Supplemental Materials

Optical properties and structural phase transitions of W-doped VO₂(R) under pressure

Huafang Zhang^a, Zhou Guan^a, Benyuan Cheng^b, Quanjun Li^{a*}, Ran Liu^a, Jing Zhang^a,
Xianzhen Liu^c, Ke Yang^d, Tian Cui^a, Bingbing Liu^{a*}

^aState Key Laboratory of Superhard Materials, Jilin University, Changchun 130012, China

^bChina Academy of Engineering Physics, Mianyang, Sichuan, 621900, China

^cU2A Beam line, Carnegie Institution of Washington, Upton, New York 11973

^dChinese Academy Sciences, Shanghai Institute Applied Physics, Shanghai 201204, Peoples R China

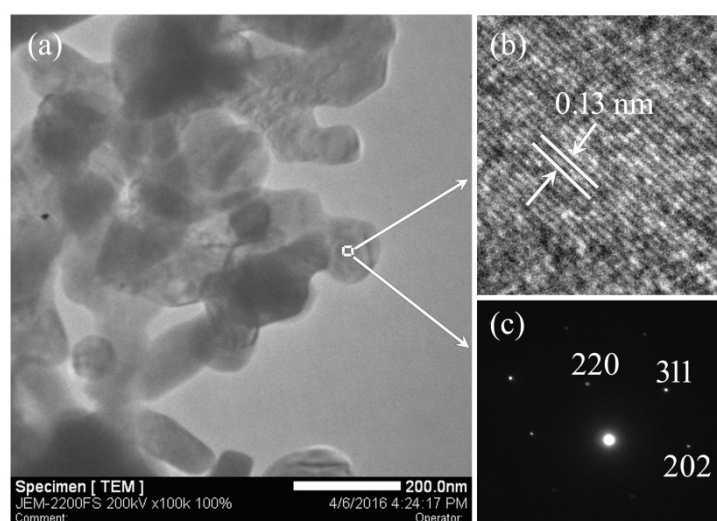


Fig. S1. (a) Typical TEM image, (b) HRTEM image and (c) SAED pattern of the W-VO₂(R) nanoparticles.

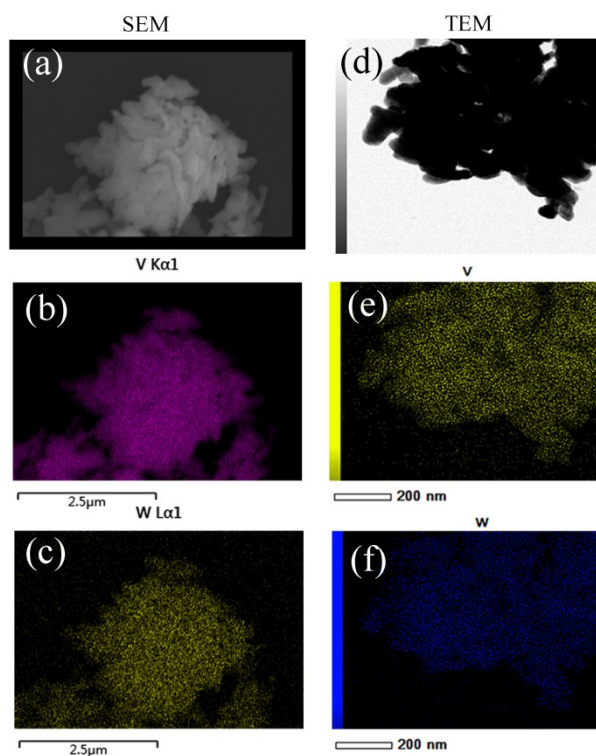


Fig. S2. The Element-Mapping of W-VO₂ nanoparticles. In SEM study (a) SEM image, (b) V-Mapping, (c) W-Mapping. In TEM study (d) TEM image, (e) V-Mapping, (f) W-Mapping. Both the SEM and TEM studies show that the relative concentration of W in the VO₂ nanoparticles is about 0.11.

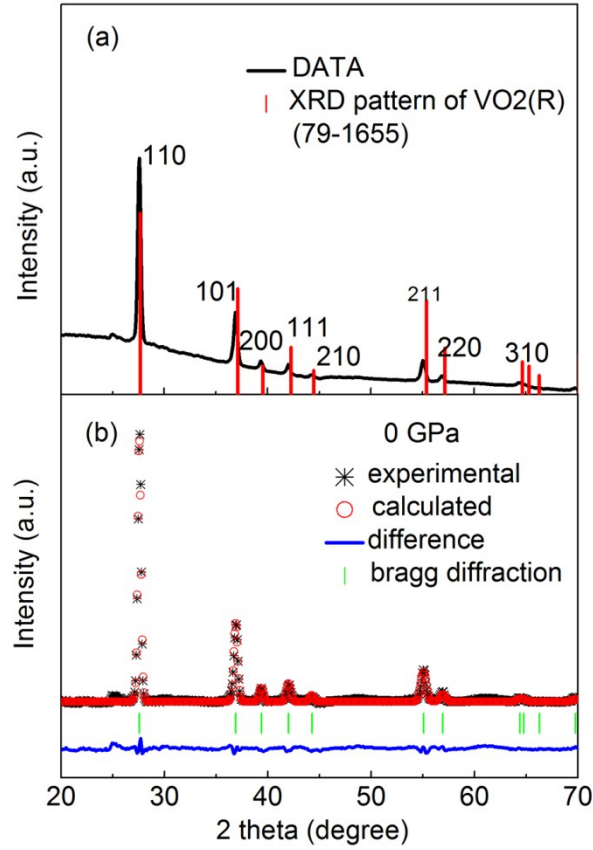


Fig. S3. (a) XRD diffraction pattern and (b) corresponding refinement results for W-VO₂(R) nanoparticles at ambient condition. The lines at the bottom of (a) correspond to the diffraction peaks of VO₂(R) taken from PDF No.79-1655.

Table S1. Lattice parameters of W-VO₂(R) and pure VO₂.

Phase	a/b(Å)	C(Å)	V(Å ³)	Reference
W-VO ₂ (R)	4.57	2.88	60.12	This study
VO ₂ (R)	4.55	2.86	59.22	PDF No.79-1655

Fig. S1 shows the typical TEM, HRTEM images and corresponding SAED pattern of the synthesized W-VO₂(R) nanoparticles with diameters of about 100nm-200nm. Fig. S2 shows elements mapping on W-VO₂(R) nanoparticles by both TEM and SEM systems. Both of these results demonstrate that the W element is homogeneously doped in samples and the “relative” concentration of W in the VO₂ sample is about 0.11. Fig. S3(a) show the XRD diffraction pattern at ambient condition, all the peaks can be indexed to VO₂(R) but with smaller angles values. We fitted the diffraction pattern with a tetragonal structure (P42/mnm) by using with

GSAS (Fig. S2(b)). The fitting gives relatively satisfying results, and the obtained lattice parameters are shown in S table1. The c-axis lattice constant against the composition x in $V_{1-x}W_xO_2$ agrees well with that of $V_{1-x}W_xO_2$ powder samples reported by Israelsson et al. (Mater. Res. Bull. 5, 19, 1970) (Fig. S4). Fig. S5 show the DSC curves of W-VO2 with only one peak centered at -26.83°C , indicating that the M1 to R transition occurs at about -26.83°C , and further verifying the uniformity of W doping.

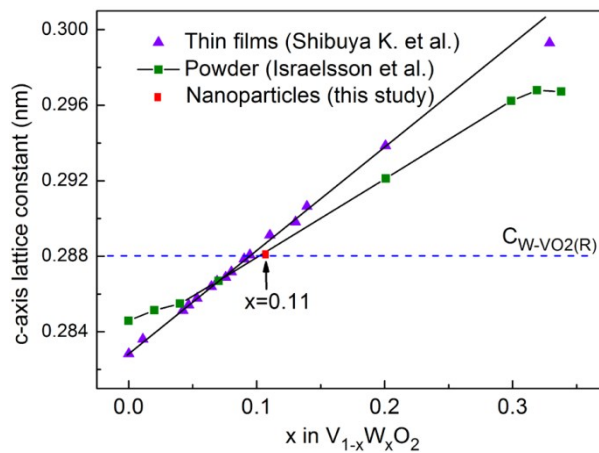


Fig. S4. Out-of-plane lattice constant against the composition x in $V_{1-x}W_xO_2$. The c-axis lattice constants of $V_{1-x}W_xO_2$ powder samples reported by Israelsson et al. (Mater. Res. Bull. 5, 19, 1970) (green square) and thin films reported by Shibuya K. et al. (Applied physics letters, 2010, 96, 022102) (purple triangle) are plotted for comparison.

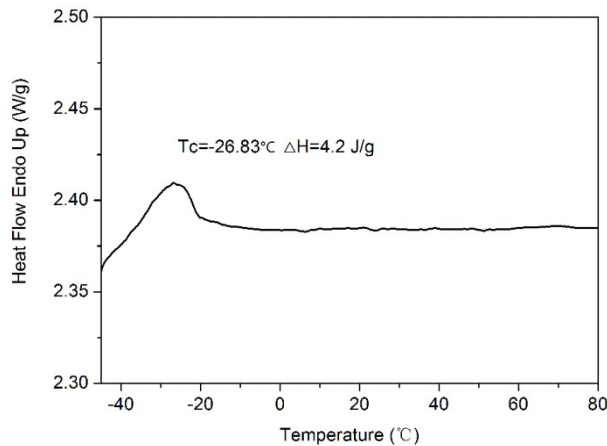


Fig. S5. DSC curves of W-doped VO2 nanoparticles.

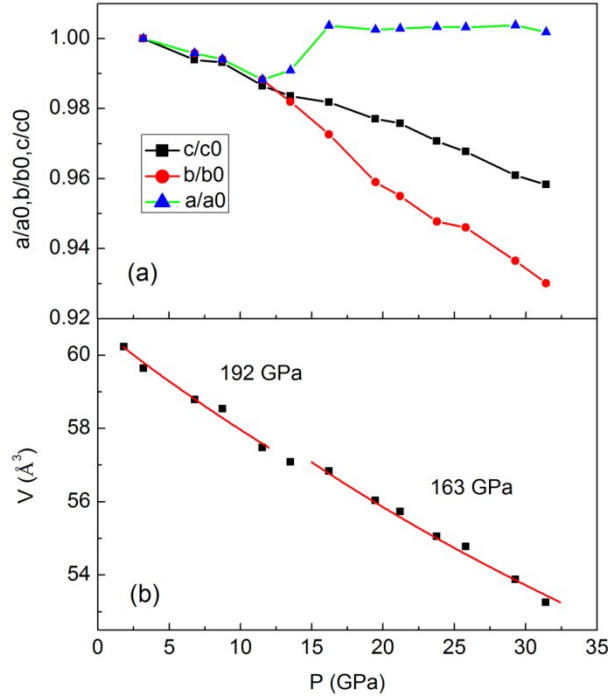


Fig. S6. (a) Pressure-relative lattice parameters diagram and (b) pressure-volume diagram of the R and CaCl_2 -type phases in W- VO_2 nanoparticles.

The pressure-relative lattice parameters diagram of the R and CaCl_2 -type phases for W- VO_2 nanoparticles are shown in Fig. S6a. In R phase, the relative lattice parameters, a , b and c , show similar compressibility. In CaCl_2 -type phase, the b axis exhibits a continuous decrease under pressure, whereas the a axis becomes nearly incompressible and the c -axis becomes more compressible, suggesting a remarkable anisotropic compression in a - c plane. The pressure-volume data of R and CaCl_2 -type phases in W- VO_2 nanoparticles are shown in Fig. S6b, and were fitted to the Birch-Murnaghan equation of state

$$P = \frac{3B_0}{2} \left[\left(\frac{V}{V_0} \right)^{-\frac{7}{3}} - \left(\frac{V}{V_0} \right)^{-\frac{5}{3}} \right] \left\{ 1 + \frac{3}{4} (B_0' - 4) \left[\left(\frac{V}{V_0} \right)^{-\frac{2}{3}} - 1 \right] \right\}$$

Where B_0 is bulk modulus, B_0' is the pressure-derivative of bulk modulus and fixed to 4, V_0 is the unit-cell volume at ambient pressure. The best-fit curves are shown in Fig.6b. The obtained bulk modulus for R and CaCl_2 -type phases for W- VO_2 nanoparticles are 192 and 163 GPa, respectively. CaCl_2 -type phase exhibits a lower bulk modulus than that of R phase, indicating the increased compressibility in CaCl_2 -type

phase, which could be associated with the anisotropic compression in a-c plane. Moreover, the bulk modulus for R and $CaCl_2$ -type phases in W-VO₂ nanoparticles is close to those of their pure counterparts (190 and 171 GPa, respectively), suggesting that partial substitution of V atoms by W atoms will not affect the lattice stability of R and $CaCl_2$ -type phases under pressure.